Journal of Applied Polymer Science

Flame Retardant and Mechanical Properties of Epoxy Composites Containing APP–PSt Core–Shell Microspheres

ChunXia Zhao,[1,2,3] YunTao Li,[1,2,3] YunLiang Xing,[2] Da He,[2] Jie Yue[2]

[1]State Key Lab of Oil & Gas Reservoir Geology and Exploitation, Southwest Petroleum University, Chengdu 610500, People's Republic of China

[2]Department of Materials and Engineering, Southwest Petroleum University, Chengdu 610500, People's Republic of China

[3]New Energy Center, Southwest Petroleum University, Chengdu 610500, People's Republic of China

Correspondence to: Y. Li (E-mail: yuntaoli@swpu.edu.cn)

ABSTRACT: Ammonium polyphosphate (APP)–polystyrene (PSt) core–shell microspheres (CSPs) were synthesized via *in situ* radical polymerization. The core–shell structure was confirmed by transmission electron microscope (TEM). The results of optical contact angle measurements demonstrated a significant improvement in hydrophobicity of the modified APP. The obtained APP–PSt CSPs were added into epoxy (EP) system with various loadings. Effects of CSP on flame retardancy, thermal properties, heat release rate (HRR), smoke production, and mechanical properties of EP/CSP composites were investigated by limiting oxygen index (LOI), UL-94 tests, thermogravimetric analysis (TGA), cone calorimeter, and tensile test. LOI and UL-94 indicated that CSP remarkably improved the flame retardancy of EP composites. TGA showed that the initial decomposition temperature and the maximum-rate decomposition temperature decreased, whereas residue yields at high temperature increased with the incorporation of microspheres. Cone calorimetry gave evidence that HRR, peak release rate, average HRR, and smoke production rate of EP/CSP composites decreased significantly. The morphology of char residues suggested that CSP could effectively promote EP to form high-quality char layer with compact outer surface and swollen inner structure. Tensile strength of EP was enhanced with the addition of CSP. © 2013 Wiley Periodicals, Inc. J. Appl. Polym. Sci. **2014**, *131*, 40218.

KEYWORDS: thermosets; flame retardance; mechanical properties; thermal properties

Received 23 July 2013; accepted 20 November 2013

DOI: 10.1002/app.40218

INTRODUCTION

Epoxy (EP) resins are used in adhesive, coating, laminating, and casting fields due to their excellent properties, such as dimensional stability, good mechanical properties, and chemical resistance. However, the flammability of epoxies has limited their applications where flame retardancy is required. Phosphorus-containing compounds, including phosphorus-containing curing agents,[1,2] reactive comonomers,[3,4] and physical doping additives,[5,6] are widely used in flame retardant EP resins. EP resins cured with amidogen groups containing a large amount of hydroxyl and nitrogenous groups are always considered as both carbonization agent and blowing agent for intumescent char formation. Due to its high phosphorus content, ammonium polyphosphate (APP) is particularly useful as a low-cost physical doping flame retardant additive for polymers. Furthermore, APP yields phosphoric acid at moderate temperature so that it could act as an acid catalyst, which is essential to generate intumescent flame retardancy during the combustion of the materials. However, the hydrophilicity of APP makes it poorly compatible with polymer matrices, which always cause some issues such as migration and hygroscopicity.[7]

Microencapsulation has been defined as a technology of packaging solids, liquids or gaseous materials in miniature and sealed capsules. Microcapsules are flexible in structure design to satisfy various performance requirements. Mechanical and physicochemical methods are mostly used for microencapsulation. Due to its relatively simple and controllable process, physicochemical method has been applied to prepare capsule materials such as polyurethane/urea[8,9] or polyamide[10] encapsulating various types of flame retardants. Interfacial polycondensation and radical polymerization are two typical physicochemical methods for encapsulation. Bourbigot and colleagues[11,12] prepared polyurethane microcapsules encapsulating diammonium hydrogen phosphate (DAHP) through interfacial polycondensation. The obtained products exhibit much better thermal stability and intumenscent behavior than pure DAHP. Recently, the same research group has developed several approaches including interfacial polymerization, solvent evaporation, coacervation,

and *in situ* polymerization, to microencapsulate DAHP with various types of polymeric capsules.[13] Ni et al.[14] achieved the microencapsulation of APP (MCAPP) by *in situ* polymerizing pentaerythritol and 2,4-toluence diisocyanate in the presence of APP. Some other efforts have been made for MCAPP with urea-melamine-formaldehyde or melamine-formaldehyde and polyurethane.[15–17] It has been proved that encapsulating of APP is an efficient way to overcome the issues such as compatibility, thermal stability, and moisture sensitivity of APP for its intumescent flame retardant applications.[18–20] However, few attentions have been paid to the synthesis of capsule with core–shell sphere morphology. It is well known that core–shell microspheres (CSPs) could provide reinforcement effect for thermosetting resins.[21]

One aim of this study is to prepare novel microspheric core–shell particles by polystyrene (PSt) encapsulating APP via *in situ* radical polymerization based on styrene (St) and APP. Another aim is to detect the effect of such CSPs on the flame retardancy and mechanical properties of EP. Structure and properties of APP-PSt CSPs were characterized by FTIR, transmission electron microscope (TEM), and contact angle measurement. The performance of APP-PSt CSPs as a flame retardant in EP system was evaluated by limiting oxygen index (LOI), UL-94, thermogravimetric analysis (TGA), and cone calorimeter. Mechanical properties of composites were tested in detail.

EXPERIMENT

Materials

APP purchased from Tongli Chemical Corp. (Chengdu, China), 2,2′-azobisisobutyronitrile (AIBN), styrene (St), poly(N-vinyl pyrrolidone) (PVP, $M_w = 30{,}000$), and absolute ethanol obtained from Kelong Chemicals (Chengdu, China) were used as the initiator, monomer, steric stabilizer, and dispersion medium, respectively. The EP resin (diglycidyl ether of biphenol A) with epoxide equivalent weight of 227 g eq^{-1} (E-44) was supplied by Wuxi Resin Factory of Blue Star New Chemical Materials Co. (Jiangsu, China). The hardener, polyethylenepolyamine was provided by Chang Zheng Huabo Co. (Chengdu, China).

Synthesis of APP-PSt CSPs

Micro-size APP-PSt spheres were prepared by *in situ* radical polymerization. Briefly, 100 mL ethanol was used as the dispersion medium, 0.7 g PVP was added as a stabilizing agent, 8 g APP, and 24 g styrene was simultaneously added into a 250-mL four-neck round-bottom flask equipped with mechanic stirrer and reflux condenser. Initiator solution (0.02 g AIBN and 20 mL ethanol) was slowly introduced into the above system. The *in situ* radical polymerization reaction of St on APP surface was performed at 70°C for 5 h with an agitation of 300 rpm. Finally, the microspheres were purified by successive centrifugation, decantation, and dispersion for 4–5 times with ethanol. The microspheres were then dried at 60°C for 8 h, followed with vacuum drying at 70°C for 12 h. Mass percentage of the shell in APP-PSt microspheres was 49.3% calculated by toluene extraction. The contrast sample, pure PSt microsphere, was prepared in the same way except the introduction of APP in polymerization process.

Preparation of EP and Flame Retardant EP Composites

The 2 g APP-PSt CSPs were added to the mixture of 84 g EP (E-44) and 14 g curing agent (polyethylenepolyamine), while stirring with a mechanical mixer for 10 min and ultrasonic dispersion for 20 min to obtain uniformly dispersed resin mixture. The resin mixture was then degassed and poured into Teflon preformed mold. The mixture was cured at 60°C for 3 h, 80°C for 2 h, and 100°C for 2 h, then EP/CSP 2% flame retardant composites was obtained. EP and EP composites with 5, 10, 15, 20 wt % CSP, 7.6 wt % APP, and 7.4 wt % PSt were prepared in the same method. The EP composites with 7.6 wt % APP and 7.4 wt % PSt were the contrast samples.

Instrumetal Analysis and Measurements

Infrared spectra were recorded on a Nicolet FTIR 6700 apparatus using a thin film with a sample to KBr ratio of 1 : 100 by mass.

The morphology and size of the CSPs, pure APP, and PSt microspheres were characterized by TEM using a JEOL H-600IV (Hitachi, Japan) microscope with an acceleration voltage of 100 kV. The samples were dyed with phosphotungstic acid before test.

The static contact angles were obtained by depositing deionized (DI) water droplets on a flat and horizontal sample surface through an optical contact angle measuring system (OCA, Dataphysics, Germany). The droplet size was adjusted by means of a microsyringe coupled to a programmable pump with slow (typically 5 μL min^{-1}) injection speed to keep the three-phase contact in equilibrium. Images of the droplets were digitized and analyzed with software to determine the contour of the drop and evaluate the contact angles on both sides of the drop. Three measurements on different areas of the sample surface were conducted and averaged.

Tensile tests were measured using a WDW-1000 universal material testing machine (Tianjing, China). The tensile tests were conducted at a displacement rate of 1 mm min^{-1} at room temperature according to the ISO 527-1 standard test method.

LOI was measured on a HC-2C oxygen index meter (Jiangning, China) with sheet dimension of 130 mm × 6.5 mm × 3.2 mm, according to ASTM D2863-97. The UL-94 rating was tested on a CFZ-2-type instrument (Jiangning, China) according to the UL-94 (ASTM D3801) with sheet dimensions of 125 mm × 12.7 mm × 3.2 mm (±0.1).

TGA was performed on a NETZSCH 209 F1 (Germany) thermal analyzer. The samples for EP and EP/CSP composites with mass 3.5 ± 0.2 mg were heated from room temperature to 700°C at 20°C min^{-1} under air.

Cone calorimeter tests were performed by using an UK device according to Fire Testing Technology ISO 5660 at an incident flux of 35 kW m^{-2}. The size of specimens was 100 mm × 100 mm × (3.2 ± 0.1) mm. The photographs of the residual chars after the cone calorimeter tests were collected by a digital camera.

RESULTS AND DISCUSSIONS

Characterization of APP-PSt CSPs

FTIR Analysis. FTIR spectra of APP and modified APP are shown in Figure 1. For the FTIR spectra of APP, the peaks at

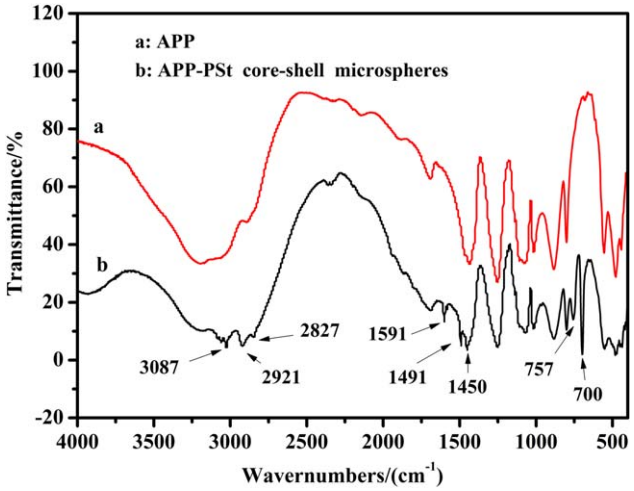

Figure 1. FTIR spectrum of APP and APP-PSt core–shell microspheres. [Color figure can be viewed in the online issue, which is available at wileyonlinelibrary.com.]

3400–3030 cm^{-1} are assigned to the asymmetric stretching absorption of NH_4^+, and 1430–1390 cm^{-1} are relevant to the bending absorption of NH_4^+. The region of 1100–850 cm^{-1} corresponding to stretching vibration of P–O–P and 1350–1100 cm^{-1} to the stretching vibration of P═O are typical fingerprint bands of polyphosphate chains.[22] The FTIR spectrum reveals the absorption peaks of PSt after microencapsulation. The stretching peaks of C–H bond in benzene ring and ethenyl appear at 3087, 2921, and 2827 cm^{-1}, respectively.[23] The absorption peaks at 1450, 1491, and 1595 cm^{-1} are attributed to the benzene ring vibration of monosubstitution. The out-of-plane deformation vibration of C–H in monosubstitution benzene ring can be seen at 753 and 700 cm^{-1}.

TEM of APP-PSt CSMs. Transmission electron micrograph of CSPs and contrast samples are shown in Figure 2. Compared with the TEM morphologies of APP and pure PSt microspheres, a typical core-shell structure with smooth surface is observed, which is proved by the sharp contrast between the dark edge and the pale center in Figure 2. The size range of these CSPs is around 0.75–2.5 μm. Combination with the analysis of FTIR, it can be confirmed that APP is well coated with PSt to form APP-PSt CSPs.

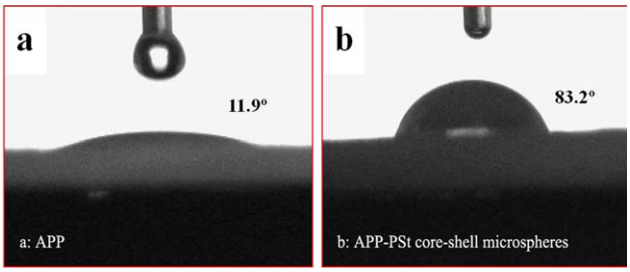

Figure 3. Contact angle of a water drop deposited on (a) APP and (b) APP-PSt core–shell microspheres. [Color figure can be viewed in the online issue, which is available at wileyonlinelibrary.com.]

Static Contact Angle Analysis. The advancing contact angle, which is sensitive to the hydrophobic moieties, has been found to be associated directly with water resistance.[24] The advancing contact angle of a water drop deposited on the unmodified APP blade surface is 11.9° [Figure 3(a)] with the droplet height of 0.22 mm after infiltration. It is clearly shown in Figure 3(b) that the water droplet sticks firmly onto the APP-PSt CSPs, and the advancing contact angle increases to 83.2° with a higher droplet height 0.95 mm. The contact angle of PSt is 82 ± 1.4° according the published work.[25] This means that PSt effectively shelled APP to form CSPs. The above results suggest that APP-PSt CSPs have hydrophobic surfaces, which could overcome APP's water-swelling issue for flame retardant applications.

Thermal Behaviors of EP and EP/CSP Composites

The TGA was used to investigate the thermal decomposition behavior of EP/CSP composites. The TGA and derivative (DTG) curves recorded in air were shown in Figures 4 and 5, respectively. The thermogravimetric data are summarized in Table I. The initial decomposition temperature ($T_{initial}$) is referred to the temperature at which the weight loss is 5 wt %.[26] The temperature of the maximum mass loss rate is labeled as T_{max}.[26,27]

There are two main stages of thermal oxidative degradation for EP and EP/CSP composites. The first stage for EP is 321–475°C corresponding to a strong DTG peak at 365°C due to the release of small-molecule degradation products.[28] The second main degradation stage, 480–700°C with T_{max} at 565°C, is mainly related to the oxidation of the remaining carbonaceous char layer with only 4.4% residue remained at 600°C. Small

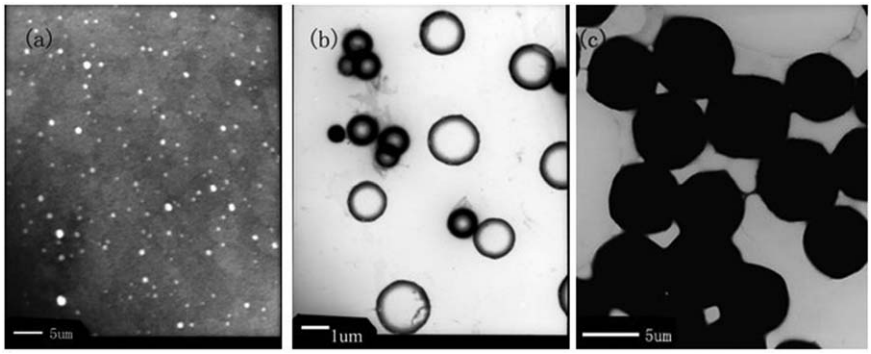

Figure 2. TEM of (a) APP, (b)APP-PSt core–shell microspheres, and (c) PSt microspheres.

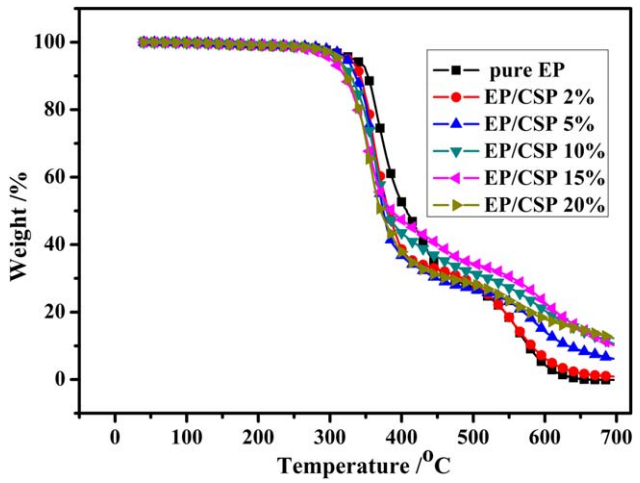

Figure 4. TGA curves of pure EP and EP/CSP composites in air. [Color figure can be viewed in the online issue, which is available at wileyonlinelibrary.com.]

amount of CSP loading can lower the initial temperature of decomposition obviously, as shown in Table I. It is noticed that the char yields of EP/CSP composites increase over 220% than that of the neat EP. Interestingly, we observed that EP/CSP 15% exhibited the lowest $T_{initial}$ and T_{max1} and the highest T_{max2} with the highest amount of char residues. Less-stable O═P–O bond in APP leads to lower $T_{initial}$ of EP/CSP composites. When heated, the groups containing phosphorus decompose to react with EP or PSt, which can accelerate the degradation of EP composite to form stable char. The shoulder attached peak to 365°C decreased with increasing CSP amount due to the accelerated degradation process by phosphorus containing flame retardant agent.[29] The stable char residue can resist the heat and substance transfer, thus preventing the further decomposition and raising the second decomposition temperature to a higher level. Phosphorous content is essential in the above char formation process. Suitable phosphorous content can favor the formation of the chars with compact surface structure but relatively loose inside, which efficiently improves the flame retardancy of the resins.[30] Similarly, excessive loading of CSP could not bring positive effect on flame retardancy to EP. EP/CSP 15% with appropriate phosphorous content owns the best char formation ability and generates the most stable char structures at high temperature.

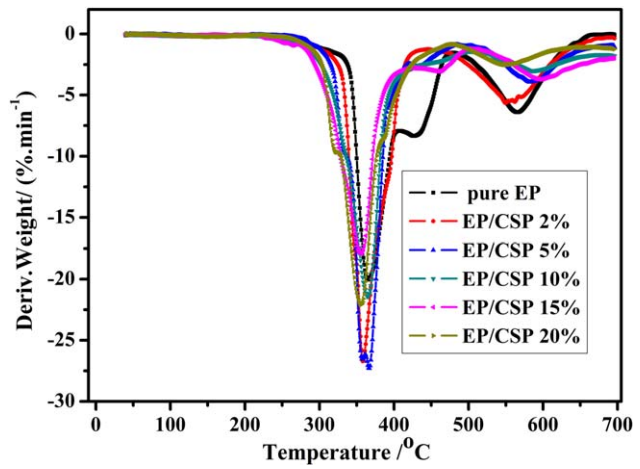

Figure 5. DTG curves of pure EP and EP/CSP composites in air. [Color figure can be viewed in the online issue, which is available at wileyonlinelibrary.com.]

Table I. TGA Data of Pure EP and EP/CSP Composites

Sample	$T_{initial}$[a] (°C)	T_{max1}[b] (°C)	T_{max2}[b] (°C)	Char residue (%) 500°C	Char residue (%) 600°C
Pure EP	332	365	566	27.3	4.4
EP/CSP 2%	325	358	564	28.4	6.4
EP/CSP 5%	324	367	581	26.8	14.3
EP/CSP 10%	310	365	590	31.5	20.5
EP/CSP 15%	301	355	597	34.5	22.9
EP/CSP 20%	313	356	551	28.3	18.0

[a] $T_{initial}$ is the initial degradation temperature (temperature at 5 wt % loss).
[b] T_{max} is the maximum-rate degradation temperature.

Flame Retardancy

Limiting Oxygen Index. The influence of APP-PSt CSPs (CSP) on the flame retardancy of EP was investigated by UL-94 vertical testing and LOI. The results of LOI and UL-94 test are shown in Table II. The flame retardant EP composites with 2, 5, 10, 15, and 20 wt % of APP-PSt CSPs by mass were labeled as EP/CSP 2%, EP/CSP 5%, EP/CSP 10%, EP/CSP 15%, and EP/CSP 20%, respectively. The contrast EP composites with 7.4 wt % PSt and 7.6 wt % APP were labeled as EP/PSt 7.4% and EP/APP 7.6%, respectively. The flame retardancy of the EP resins was significantly improved with the loading of CSP. No char layer formed for neat EP and EP/PSt during the LOI and UL-94 testing. The thermally decomposing surface was exposed directly to fire and propagated quickly to the fixture. UL-94 rate is N.R. LOI value is just 23.2 for EP/CSP 2%, but dripping is no longer observed. For EP composites loaded with 5 wt % and above of CSP, self-extinguishing can be detected and the burning time are significantly decreased. The LOI value levels up to 28.5 with 15 wt % loading. The LOI value increases slightly for EP/CSP 20% sample. The results may suggest that the best loading amount of APP-PSt CSPs exists for flame retardant EP

Table II. LOI and UL-94 Test Results of EP and EP/CSP Composites

Sample	LOI	UL-94	t_1 (s)	t_2 (s)	Dripping
EP	22.0	N.R.	-	-	Yes
EP/CSP 2%	23.2	N.R.	-	-	No
EP/CSP 5%	25.7	V-1	43	26	No
EP/CSP 10%	26.3	V-1	24	11	No
EP/CSP 15%	28.5	V-1	15	5	No
EP/CSP 20%	28.7	V-1	22	9	No
EP/PSt 7.4%	19.7	N.R.	-	-	Yes
EP/APP 7.6%	28.6	V-1	13	4	No

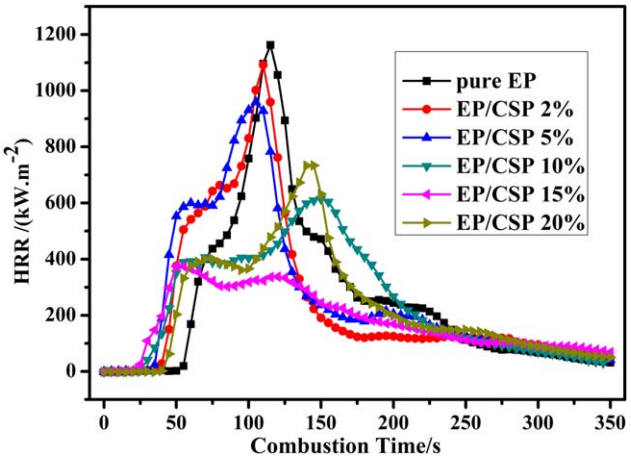

Figure 6. Effects of CSP loading on heat release rate of EP. [Color figure can be viewed in the online issue, which is available at wileyonlinelibrary.com.]

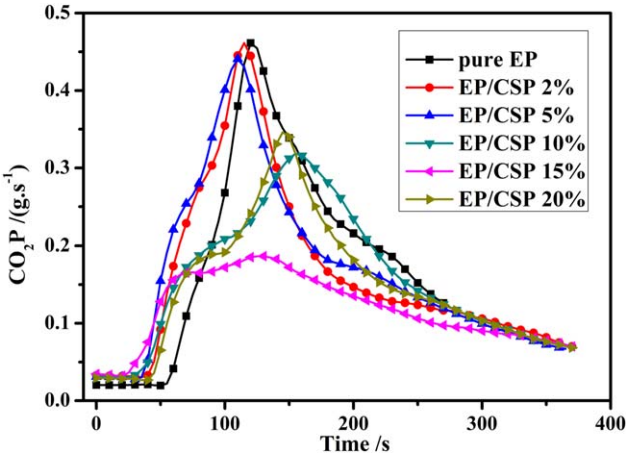

Figure 8. CO_2 production (CO_2P) as a function of time. [Color figure can be viewed in the online issue, which is available at wileyonlinelibrary.com.]

composite with CSP 15%. The LOT value and UL-94 rate of EP/APP 7.6% is similar with that of EP/CSP 15%, which means the contribution of APP in CSP on the flame retardant properties. According to UL-94 test results, the second burning times (t_2) of EP composites with 5–20 wt % of CSP are extremely shorter than the first ones (t_1). Therefore, we can conclude that the effective protection of char layer formed on EP/CSP composites during the first combustion section.

Cone Calorimetry. Cone calorimetry (CONE) is one of the most effective methods to evaluate the flammability characteristics and potential fire safety of materials under well-ventilated conditions.[31] The heat release rate (HRR), smoke production rate (SPR), CO_2 production (CO_2P), and CO production (COP) are shown in Figures 6–9, respectively. Table III shows the results of peak values of heat release (PHRR), average HRR (AHRR), total heat release (THR), time into ignition (TTI), and total smoke rate (TSR).

Pure EP burnt very fast after ignition and a sharp peak appears at 1163.1 kW m^{-2}. The introduction of CSP in EP decreases the HRR values significantly as shown in Figure 6. The HRR curves of EP/CSP composites changed to two obviously broad PHRRs instead of one peak for EP. The first PHRR ($PHRR_1$) of EP/CSP 2% is about 731.3 kW m^{-2}. $PHRR_2$ of EP/CSP 2% is 1009.2 kW m^{-2}, which is quite similar with the PHRR value of EP. Combined with the results from TGA, it can be deduced the first PHRR for EP/CSP composites is mainly related with the decomposition or combustion of CSP. EP/CSP 15% has the lowest PHRR value among EP/CSP composites. It has $PHRR_1$ of 375.4 kW m^{-2} and $PHRR_2$ of 337.3 kW m^{-2}, which is approximately one third of PHRR of EP. HRR and PHRR are considered as the most important parameters to evaluate fire safety of flame retardant materials. These parameters demonstrate the rate of fuel feeding in the combustion and the further rate of flame spread.[32] Commonly, a lower PHRR corresponds to a slower flame spread and less fire hazard. It is clear that CSP can effectively reduce the HRR of EP and slow down the flame propagation. During the test, virgin EP releases a total heat of 90.3 MJ m^{-2}, whereas the EP/CSP 15% releases 65.7 MJ m^{-2}. The reduction in HRR is mainly due to the physical isolation as reported in the literatures.[33] The AHRR of EP is reduced significantly by the incorporation of CSP (Table III). With

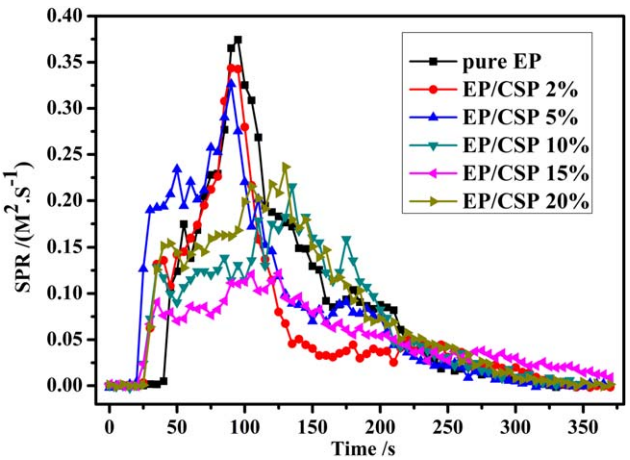

Figure 7. Smoke production rate (SPR) as a function of time. [Color figure can be viewed in the online issue, which is available at wileyonlinelibrary.com.]

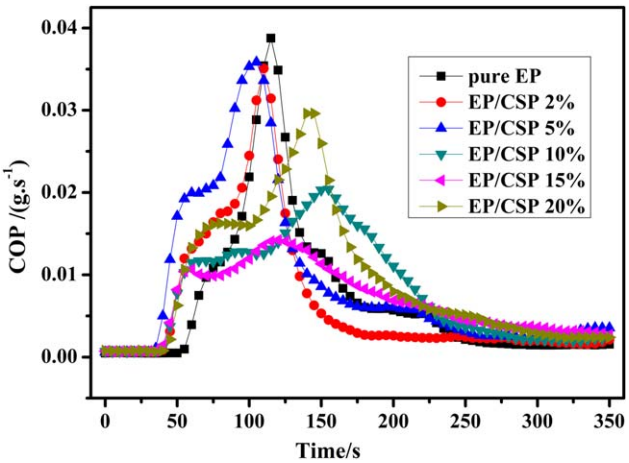

Figure 9. CO production (COP) as a function of time. [Color figure can be viewed in the online issue, which is available at wileyonlinelibrary.com.]

Table III. Detailed Combustion Results of Neat EP and EP/CSP Composites Obtained From Cone Calorimetry

Samples	$PHRR_1$ (kW m^{-2})	$PHRR_2$ (kW m^{-2})	AHRR (kW m^{-2})	TTI (s)	THRR (MJ m^{-2})	TSR (m^2 m^{-2})
EP	-	1163.1	284.8	40	90.3	3499.5
EP/CSP 2%	731.3	1092.2	274.9	21	86.4	2812.9
EP/CSP 5%	600.1	959.5	272.5	20	92.6	3447.8
EP/CSP 10%	392.3	614.2	254.9	10	85.8	3006.9
EP/CSP 15%	375.4	337.3	185.8	8	65.7	2247.7
EP/CSP 20%	400.8	733.7	237.6	25	81.7	3397.5

15 wt % CSP in the system, AHRR value of EP composite decreased from 284.8 to 185.8 kW m^{-2}. Combined with the higher char residue of EP/CSR composites, the lower THR and AHRR values suggest that EP/CSR composites may partially undergo a char-formation process rather than combustion during the burn test.[34]

Smoke performance of flame retardant material is also important in fire safety evaluation.[35] The peak values of EP's SPR decrease greatly with the addition of CSP. Compared with the SPR peak value of pure EP system, those values of EP/CSP 10% and EP/CSP 15% are reduced by factors of 47 and 233%, respectively. However, during the test period between 20s and 50s, the SPR values of the EP/CSP composites are higher than that of the pure EP. This phenomenon is caused by the decomposition of phosphate ester in APP at relatively low temperature. The production rates of CO_2 and CO are lowered obviously during combustion as shown in Figures 8 and 9, indicating that addition of CSP can reduce both flammability and fire toxic gases of EP. The TSR values of EP composites also decreased compared to pure EP system (Table III). CSP exhibited great smoke suppression effect on EP composites. Certain amount of CSP loading can promote charring and enhance the char quality, which can protect the inner matrix and reduce the amount of smoke-forming materials in the gas phase.

It is worthy to note that the TTI of EP/CSP composites is shorter than that of pure EP. The TTI value of EP/CSP 15% is only 8s, much lower than the value of 40s for pure EP. It is mainly caused by flammable volatile molecules produced from the decomposition of PSt shell at the earlier stage, for the LOI of PSt is around 17.5.[36] Interestingly, the results of LOI, UL-94, TG, and CONE are in good accordance to demonstrate the best flame retardant properties of EP/CSP 15%. Therefore, it is necessary to investigate the char morphology after CONE calorimetry test so that a possible char formation mechanism could be obtained.

Morphology of Char Residues

The high-quality char can act as an insulating barrier during degradation, which can limit the diffusion of volatiles to the flame zone. The analysis of char layers can provide insight into fire resistant performance, and further reveal possible char-forming process for flame retardant materials.[37] The integral morphology of the char residues of EP and EP/CSP composites after CONE calorimetry tests are illustrated in Figure 10. The pure EP is entirely burnt out. Contrarily, instumescent char layers are clearly seen for EP/CSP composites even with only 2 wt % of CSP. It is obvious that CSP can promote the formation of effective charring layer. A high char yield corresponds to a strong solid-phase mechanism of EP/CSP flame retardant composites. It is observed that the residual chars of all EP/CSP

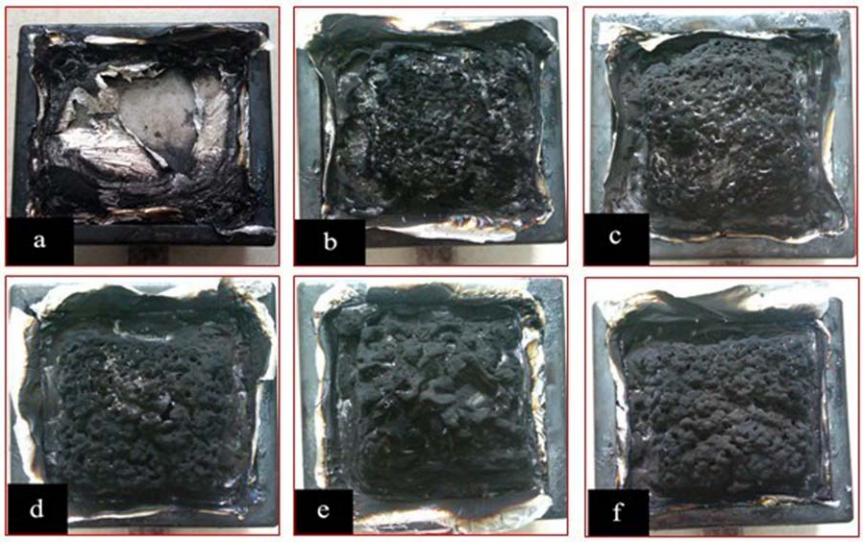

Figure 10. Photographs of the integral residues after the cone calorimeter tests: (a) Pure EP; (b) EP/CSP 2%; (c) EP/CSP 5%; (d) EP/CSP 10%; (e) EP/CSP 15%; and (f) EP/CSP 20%. [Color figure can be viewed in the online issue, which is available at wileyonlinelibrary.com.]

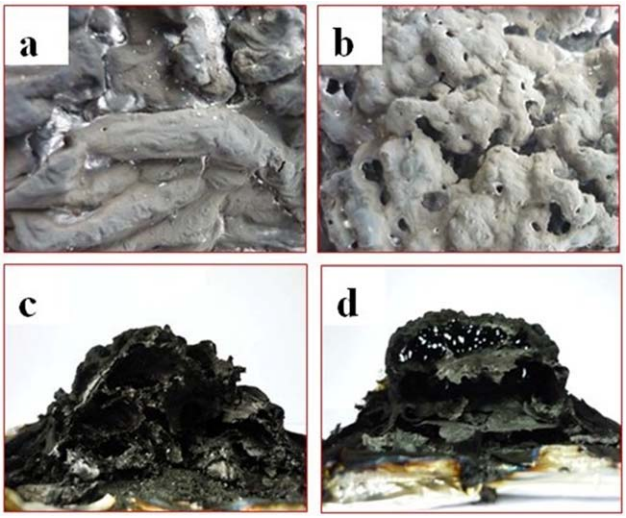

Figure 11. Photographs of outer surfaces from top view (a) EP/CSP 15% and (b) EP/CSP 20%; and internal structure from cross-section (c) EP/CSP 15% and (d) EP/CSP 20%. [Color figure can be viewed in the online issue, which is available at wileyonlinelibrary.com.]

composites are expanded significantly in volume. The porous surfaces are formed, except for EP/CSP 15%. It demonstrated that the proper loading of CSP is critical for the formation of high-quality char layer. This may be due to the synergistic effects from gas resource, cross-linking reaction in polymer degradation and the viscosity of melt mixture covered on the surface. The outer surface of char layer can be broken through, if the gas resource is excessive or the viscosity of prior degraded soften mixture is low. The surface morphology and internal structure of the chars are the pivotal roles for solid-phase flame retardant. The char layer is cut for the observation of its inner structure. Figure 11 shows the digital images of outer surface and inside structure of EP/CSP 15% and EP/CSP 20% flame retardant materials. Notably, the inner structure of EP/CSP 15% seems more consecutive and swollen with many smaller hollow cells. Meanwhile, EP/CSP 15% owns much more compact outer surface than that of EP/CSP 20% shown in Figure 11(a,b). Such structure favors the generation of temperature gradient in char layer and protects the matrix inside.[38] Outer surface of the char layer is compact enough to prevent gas penetration and to cut off oxygen from the degraded volatiles more efficiently as reported.[39,40] EP with 15 wt % of CSP can form high-quality protective char layer on the surface of composites, which serves as a good barrier against heat and oxygen diffusion.

Table IV. Mechanical Properties of EP and EP/CSP Composites

Sample	Elongation at break (%)	Tensile strength (MPa)	Young's modulus (MPa)
EP	0.38 ± 0.05	23.3 ± 0.9	2303 ± 25
EP/CSP 2%	0.43 ± 0.02	34.1 ± 1.1	2456 ± 40
EP/CSP 5%	0.42 ± 0.03	29.7 ± 0.6	2596 ± 32
EP/CSP 10%	0.46 ± 0.02	28.3 ± 0.7	2671 ± 29
EP/CSP 15%	0.50 ± 0.04	27.4 ± 0.6	2536 ± 31
EP/CSP 20%	0.41 ± 0.03	24.3 ± 0.8	2317 ± 38
EP/PSt 7.4%	0.34 ± 0.01	21.3 ± 0.4	1976 ± 32
EP/APP 7.6%	0.32 ± 0.02	20.5 ± 0.2	1893 ± 23

Mechanical Properties of EP and EP/CSP Composites

Table IV shows the results of the mechanical measurements for EP and EP/CSP composites. The tensile strength, elongation at break and Young's modulus of the pure EP were measured to be 23.3 MPa, 0.38%, and 2303 MPa, respectively. The tensile strength of EP with PSt or APP alone were decreased by factors of 8.5 and 12.0%, respectively. Considerable improvements were observed in the mechanical properties of EP upon addition of CSP. At low loading, i.e., 2 wt %, the addition of CSP is leading to increase in tensile strength, elongation at break, and Young's modulus by factors of 46.3, 13.2, and 6.6%. It is noteworthy that EP/CSP 15% owning the highest improvement in LOI value achieves notable increases of tensile strength 17.6%, elongation at break 31.5%, and Young's modulus 10.1%. The above results show the positive effect of CSPs on mechanical properties. Considering the combination properties of flame-retarded EP resin, the sample of EP with CSP 15% has the best performance.

CONCLUSIONS

Novel core–shell APP-PSt microspheres (CSP) with good water resistance properties were synthesized via *in situ* radical polymerization and characterized by FTIR, TEM, and optical contact angle measurement. The LOI value and UL-94 level of EP were greatly improved with the addition of CSP. CSP can effectively reduce the flammability of EP. Compared with pure EP system, the HRR, PHRR, AHRR, and SPR values of obtained EP/CSP composites decrease significantly, especially for EP/CSP 15%. EP/CSP 15% can achieve an LOI value of 28.5. Moreover, a higher quality char layer with compact outer surface and swollen inner structure is observed for EP/CSP 15% composite. Meanwhile, EP/CSP 15% achieves increases of tensile strength 17.6%, elongation at break 31.5%, and Young's modulus 10.1% with respect to the pure EP.

ACKNOWLEDGMENTS

The work was financially supported by the Fund of General Program of Sichuan Provincial Department of Education, China (no. 1ZB021), the Fund of Science and Technology for Youth of Southwest Petroleum University, China (no. 2012XJZ036), and Science and Technology Innovation Seedling Project of Sichuan Province (no. 2012ZZ081). Fund for Innovation Research Team of Young Scholar in Southwest Petroleum University, China (no. 2013XJZT005).

REFERENCES

1. Liu, W. C.; Varley, R. J.; Simon, G. P. *Polymer* **2006**, *47*, 2091.
2. Spontón, M.; Mercado, L. A.; Ronda, J. C.; Galià, M.; Cádiz, V. *Polym. Degrad. Stab.* **2008**, *93*, 2025.
3. Toldy, A.; Szolnoki, B.; Marosi, G. *Polym. Degrad. Stab.* **2011**, *96*, 371.
4. Liu, W. S.; Wang, Z. G.; Xiong, L.; Zhao, L. N. *Polymer* **2010**, *51*, 4776.

5. Peerez, R. M.; Sandler, J. K. W.; Altstadt, V.; Hoffmann, T.; Pospiech, D.; Ciesielski, M. *Polymer* **2007**, *48*, 778.
6. Zhang, L. L.; Liu, A. H.; Zeng, X. R. *J. Appl. Polym. Sci.* **2009**, *111*, 168.
7. Sun, C. Y.; Zhang, Q. B.; Sun, B. L. *J. Polym. Res.* **2007**, *14*, 505.
8. Zhao, K. M.; Xu, W. Z.; Song, L.; Wang, B. B.; Feng, H.; Hu, Y. *Polym. Adv. Technol.* **2012**, *23*, 894.
9. Lu, S. F.; Xing, J. W.; Zhang, Z. H.; Jia, G. P. *J. Appl. Polym. Sci.* **2011**, *121*, 3377.
10. Giraud, S.; Bourbigot, S.; Rochery, M.; Vroman, I.; Tighzert, L.; Delobel, R. *J. Ind. Text.* **2011**, *31*, 11.
11. Giraud, S.; Bourbigot, S.; Rochery, M.; Vroman, I.; Tighzert, L.; Delobel, R. *Polym. Degrad. Stab.* **2002**, *77*, 285.
12. Saihi, D.; Vroman, I.; Giraud, S.; Bourbigot, S. *React. Funct. Polym.* **2006**, *66*, 1118.
13. Giraud, S.; Salaün, F.; Bedek, G.; Vroman, I.; Bourbigot, S. *Polym. Degrad. Stab.* **2010**, *95*, 315.
14. Ni, J. X.; Song, L.; Hu, Y.; Zhang, P.; Xing, W. Y. *Polym. Adv. Technol.* **2009**, *20*, 999.
15. Saihi, D.; Vroman, I.; Giraud, S.; Bourbigot, S. *React. Funct. Polym.* **2005**, *64*, 127.
16. Ni, J. X.; Ta, Q. L.; Lu, H. D.; Hu, Y.; Song, L. *Polym. Adv. Technol.* **2010**, *21*, 392.
17. Michels, E.; Staendeke, H. *Phosphorous Sulfur* **2009**, *46*, 136.
18. Zhou, L.; Guo, C. G.; Li L. P. *J. Appl. Polym. Sci.* **2011**, *122*, 849.
19. Wang, J.; Yi, J. S.; Cai, X. F. *J. Appl. Polym. Sci.* **2011**, *120*, 968.
20. Zhou, J.; Yang, L.; Wang, X. L.; Fu, Q. J.; Sun, Q. L.; Zhang, Z. Y. *J. Appl. Polym. Sci.* **2013**, *129*, 36.
21. Jo, Y. G.; Choe, Y. S. *Mol. Cryst. Liq. Cryst.* **2011**, *539*, 190.
22. Nie, S. B.; Hu, Y.; Song, L.; He, Q. L.; Yang, D. D.; Chen, H. *Polym. Adv. Technol.* **2008**, *19*, 1077.
23. An, J.; Wang, D. S.; Luo, Q. Z.; Yuan, X. Y. *Mater. Sci. Eng. C* **2009**, *29*, 1984.
24. Cao, S. S.; Liu, B. L.; Deng, X. B.; Li, S. *J. Macromol. Biosci.* **2005**, *5*, 669.
25. Tunma, S.; Song, D. H.; Kim, S. E.; Kim, K. N.; Han, J. G.; Boonyawan, D. *Appl. Surf. Sci.* **2013**, *283*, 930.
26. Zhao, C. X.; Liu, Y.; Wang, D. Y.; Wang, D. L.; Wang, Y. Z. *Polym. Degrad. Stab.* **2008**, *93*, 1323.
27. Zhao, C. X.; Peng, G.; Liu, B. L.; Jiang, Z. W. *J. Polym. Res.* **2011**, 18, **1971**.
28. Wang, X.; Hu, Y.; Song, L.; Xing, W. Y.; Lu, H. D. *J. Anal. Appl. Pyrol.* **2011**, *92*, 164.
29. Hua, R.; Jian, Z. S.; Bin, J. W.; Qi, Y. Z. *Polym. Degrad. Stab.* **2007**, *92*, 956.
30. Wang, X.; Hu, Y.; Song, L.; Xing, W. Y.; Lu, H. D.; Lv, P.; Jie, G. X. *Polymer* **2010**, *51*, 2435.
31. Gilman, J. W.; Jackson, C. L.; Morgan, A. B.; Harris, R. *Chem. Mater.* **2010**, *49*, 6003.
32. Wang, J. S.; Liu, Y.; Zhao, H. B.; Liu, J.; Wang, D. Y.; Song, Y. P. Wang, Y. Z. *Polym. Degrad. Stab.* **2009**, *94*, 625.
33. Qian, L. J.; Ye, L. J.; Xu, G. Z.; Liu, J.; Guo, J. Q. *Polym. Degrad. Stab.* **2011**, *96*, 1118.
34. Hshieh, F. Y.; Beeson, H. D. *Fire Mater.* **2004**, *19*, 233.
35. Chen, X. L.; Jiao, C. M.; Li, S. X.; Sun, J. *J. Polym. Res.* **2011**, *18*, 2229.
36. Cullis, C. F.; Hirschler, M. M.; Tao, Q. M. *Eur. Polvm. J.* **1986**, *22*, 161.
37. Horrocks, A. R. *Polym. Degrad. Stab.* **1996**, *54*, 143.
38. Laoutid, F.; Bonnaud, L.; Alexandre, M.; Lopez-Cuesta, J. M.; Dubois, P. *Mater. Sci. Eng. R: Rep.* **2009**, *63*, 100.
39. Liu, J.; Tang, J. Y.; Wang, X. D.; Wu, D. Z. *RSC Adv.* **2012**, *2*, 5789.
40. Ge, L. L.; Duan, H. J.; Zhang, X. G.; Chen, C.; Tang, J. H.; Li, Z. M. *J. Appl. Polym. Sci.* **2012**, *126*, 1337.